JCB Article

A novel human protein of the maternal centriole is required for the final stages of cytokinesis and entry into S phase

Adam Gromley,[1] Agata Jurczyk,[1] James Sillibourne,[1] Ensar Halilovic,[1] Mette Mogensen,[3] Irina Groisman,[1] Maureen Blomberg,[2] and Stephen Doxsey[1]

[1]Department of Molecular Medicine and [2]Department of Cell Biology, University of Massachusetts Medical School, Worcester, MA 01605
[3]School of Biological Sciences, University of East Anglia, Norwich NR4 7TJ, UK

Centrosomes nucleate microtubules and contribute to mitotic spindle organization and function. They also participate in cytokinesis and cell cycle progression in ways that are poorly understood. Here we describe a novel human protein called centriolin that localizes to the maternal centriole and functions in both cytokinesis and cell cycle progression. Centriolin silencing induces cytokinesis failure by a novel mechanism whereby cells remain interconnected by long intercellular bridges. Most cells continue to cycle, reenter mitosis, and form multicellular syncytia. Some ultimately divide or undergo apoptosis specifically during the protracted period of cytokinesis. At later times, viable cells arrest in G1/G0. The cytokinesis activity is localized to a centriolin domain that shares homology with Nud1p and Cdc11p, budding and fission yeast proteins that anchor regulatory pathways involved in progression through the late stages of mitosis. The Nud1p-like domain of centriolin binds Bub2p, another component of the budding yeast pathway. We conclude that centriolin is required for a late stage of vertebrate cytokinesis, perhaps the final cell cleavage event, and plays a role in progression into S phase.

Introduction

Centrosomes are the major microtubule-nucleating organelles in most vertebrate cells (Doxsey, 2001b). In mitosis, they contribute to spindle organization and function, and in interphase, they organize microtubule arrays that serve as tracks for transporting proteins, organelles, and chromosomes. The centrosome also anchors regulatory molecules and may serve as a central site that receives, integrates, and transmits signals that regulate fundamental cellular functions. The core of the centrosome is comprised of a pair of centrioles, microtubule barrels that appear to anchor microtubules (Chretien et al., 1997; Piel et al., 2000). Each centriole is surrounded by pericentriolar material or centrosome matrix, which nucleates the growth of new microtubules and seems to be organized by the centrioles (Bobinnec et al., 1998). Although best known for their role in microtubule nucleation, recent data suggest that centrosomes also play key roles in cytokinesis and cell cycle progression.

A role for centrosomes in defining the site of cell cleavage during cytokinesis has been suggested for some time (Rappaport, 1986). Recent studies with vertebrate cells provide evidence for a direct link between centrosome activity and completion of cytokinesis. Elimination of centrosomes from interphase cells by removal with a microneedle (Hinchcliffe et al., 2001) or from mitotic cells by laser ablation (Khodjakov and Rieder, 2001) caused cytokinesis defects, arrest, or failure. In another study, it was shown that during the final stages of cytokinesis, the maternal centriole moved to the intercellular bridge, the microtubule-filled interconnection between nascent daughter cells (Piel et al., 2001). Centriole repositioning correlated with bridge narrowing and microtubule depolymerization, while movement of the centriole away from the bridge correlated with cell cleavage or abscission. The authors suggested that the maternal centriole might anchor a regulatory pathway that controls the final stages of cell division in vertebrate cells. This would be analogous to regulatory pathways anchored at spindle pole bodies (the centrosome equivalent) in budding and fission yeasts that control mitotic

A. Gromley and A. Jurczyk contributed equally to this work.

The online version of this article includes supplemental material.

Address correspondence to Stephen Doxsey, University of Massachusetts Medical School, Department of Molecular Medicine, 373 Plantation Street, Suite 206, Worcester, MA 01605. Tel.: (508) 856-1613. Fax: (508) 856-4289. E-mail: stephen.doxsey@umassmed.edu

Key words: centrosome; maternal centriole; cytokinesis; cell cycle progression; MEN/SIN

exit and cytokinesis (for reviews see Bardin and Amon, 2001; McCollum and Gould, 2001; Pereira and Schiebel, 2001). However, no vertebrate pathway analogous to the mitotic exit network (MEN)* in budding yeast or septation initiation network (SIN) in fission yeast has been identified (Glotzer, 2001; Guertin et al., 2002). Moreover, the role of centrosome-associated molecules in the process of cytokinesis is poorly understood.

In addition to their role in cytokinesis, centrosomes appear to have a role in cell cycle progression. Recent evidence demonstrates that vertebrate cells lacking centrosomes do not initiate DNA replication (Hinchcliffe et al., 2001; Khodjakov and Rieder, 2001). The authors suggested that centrosomes controlled entry into S phase by recruiting or concentrating "core" centrosome molecules required for this process or that they indirectly activated a cellular checkpoint that monitored aberrant centrosome number. In another experimental system, vertebrate cells treated with cytochalasin D to inhibit actin-mediated cell cleavage also arrested cells in G1 as binucleate cells with supernumerary centrosomes (Andreassen et al., 2001). Although these results suggest that changes in centrosome number can affect entry into S phase, the precise role of centrosomes in cell cycle progression in vertebrate cells will require identification of the molecular components and pathways that control these events.

In this paper, we identify a novel component of the vertebrate maternal centriole called centriolin. Abrogation of centriolin function by small interfering RNA (siRNA) silencing, overexpression, or antibody inhibition produces cytokinesis failure and G1/G0 arrest, just as seen when centrosomes are experimentally eliminated from cells. Centriolin silencing produces a novel cytokinesis phenotype in which dividing cells remain interconnected by long strands of cytoplasm and fail to cleave. The cytokinesis activity lies in a centriolin domain that is homologous to the MEN/SIN components Nud1p/Cdc11p and binds the Nud1p-interacting GTPase-activating protein Bub2p. We conclude that centriolin is required for a distinct step in the final stages of vertebrate cytokinesis and can influence entry into S phase.

Results

Identification and cloning of a novel protein localized to the maternal centriole and intercellular bridge

Using sera from patients with the autoimmune disease scleroderma that react with centrosomes (Doxsey et al., 1994), we screened a human placenta λgt11 cDNA expression library to identify genes encoding the autoantigens. Of the 3×10^6 clones screened, only one of 1.7 kb was identified, indicating that the mRNA for this molecule was rare. The full-length cDNA was obtained, and the protein encoded by the cDNA was called centriolin (see below and Materials and methods). The amino acid sequence of centriolin predicted a protein with several coiled-coil regions interrupted by noncoiled domains (Lupas et al., 1991) (Fig. 1 a). Two domains within the centriolin sequence shared homology with human oncogenic transforming acidic coiled-coil proteins (TACCs), which localize to centrosomes and are implicated in microtubule stabilization and spindle function (Lee et al., 2001). Another domain of centriolin was homologous to human stathmin, an oncogenic protein involved in microtubule destabilization (Andersen, 2000). The carboxy terminus of centriolin was identical to CEP110, a naturally occurring fusion to the fibroblast growth factor receptor that localizes to centrosomes, is oncogenic, and is of unknown function (Guasch et al., 2000). The relationship of CEP110 to centriolin is unknown, although we did not identify a cDNA corresponding to this protein in our library screens. A region of centriolin near the amino terminus shared homology with Nud1p and Cdc11p, budding and fission yeast spindle pole body proteins that anchor components of the yeast MEN and SIN, respectively, and are required for completion of mitosis and cytokinesis (Bardin and Amon, 2001; McCollum and Gould, 2001; Pereira and Schiebel, 2001; Guertin et al., 2002). The 120–amino acid region of shared homology between the Nud1 domain, Nud1p, and Cdc11p all have leucine-rich repeats and are predicted to form β helix structures in tertiary structure prediction programs.

Antibodies raised against recombinant centriolin recognized a band of ~270 kD on Western blots of isolated centrosome fractions, whereas preimmune sera showed no specific bands (Fig. 1 b, Centrosome fractions). In vitro translation and overexpression of the protein in mammalian cells using the full-length cDNA produced a protein with a molecular weight similar to the endogenous protein (Fig. 1 b, In vitro translated and Overexpressed) and to a protein predicted from the cDNA sequence (see Materials and methods).

Immunofluorescence microscopy demonstrated that centriolin was localized to centrosomes in a wide variety of species, including human, monkey, hamster, mouse, and *Xenopus* (Figs. 1 and 2; unpublished data). Centrosome localization was confirmed by showing that an HA-tagged centriolin protein ectopically expressed in COS cells localized to centrosomes (Fig. 2 a). The endogenous protein was present on the centrosome throughout the cell cycle. In late G1/early S phase, centrosomes begin to duplicate, and by G2/M, duplication is usually completed. During the duplication process, centriolin was present on only one of the two duplicating centrosomes, although other proteins, such as γ-tubulin, were found on both (Fig. 1 c, G2 cell). Beginning at late G2/prometaphase, dim staining was observed next to a brightly stained centrosome. By metaphase, when centrosomes become "mature," both centrosomes had equally high levels of centriolin and were more brightly stained than at any other cell cycle stage. This demonstrates that centriolin is a marker for centrosome maturation, a characteristic shared with cenexin (Lange and Gull, 1995) and ninein (Mogensen et al., 2000). At the metaphase to anaphase transition, centriolin staining diminished at centrosomes and reached its lowest levels by late anaphase/telophase. During cytokinesis, centriolin sometimes appeared as one or two dots adjacent to the intercellular bridge, suggesting that the centrosome/centriole had moved to this site (Fig. 1 c, Telo early). This staining pattern was consistent with recent time-

*Abbreviations used in this paper: MEN, mitotic exit network; RPE, retinal pigment epithelial; SIN, septation initiation network; siRNA, small interfering RNA; TACC, transforming acidic coiled-coil protein; TAD, transactivation domain.

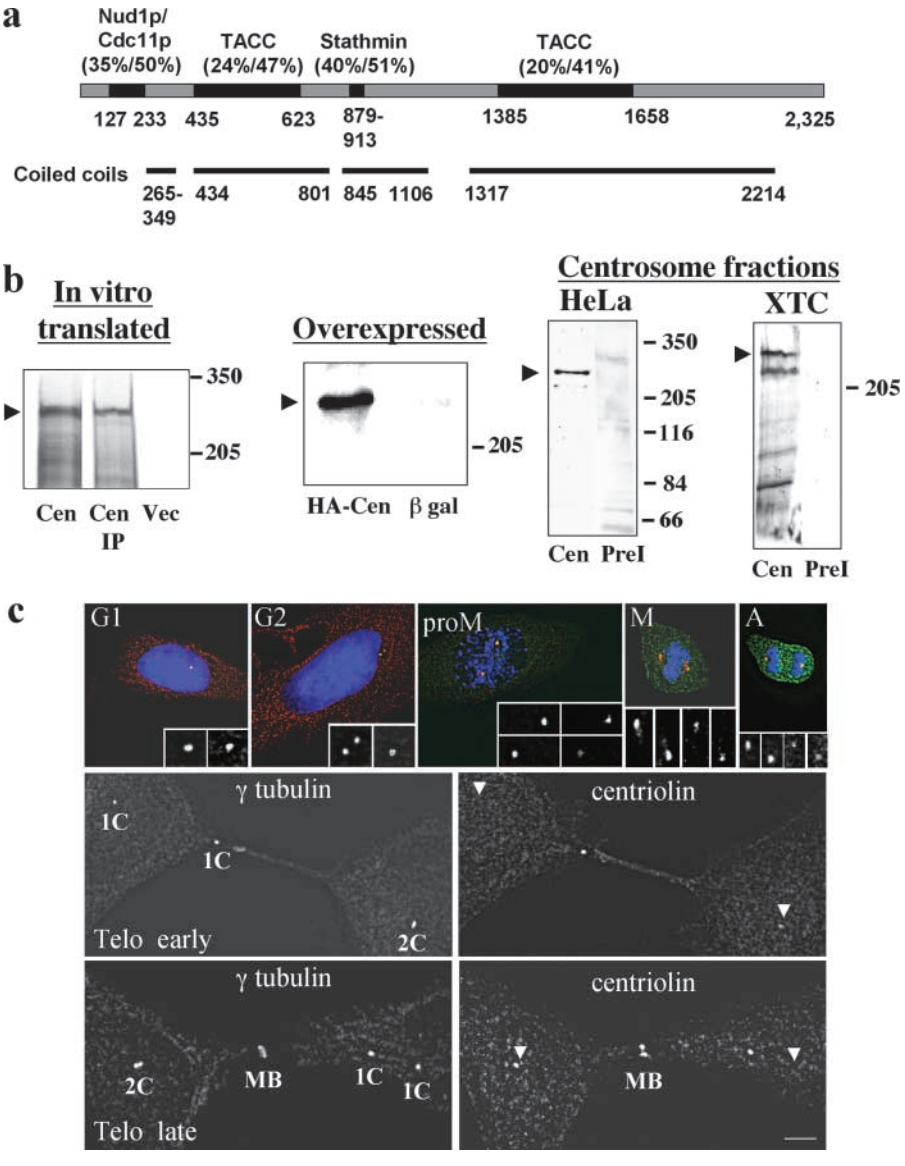

Figure 1. **Centriolin is an ~270-kD coiled-coil protein localized to mature centrosomes and the midbody.** (a, top) Schematic showing centriolin domains that share homology with budding and fission yeast proteins Nud1p and Cdc11p, human stathmin, and human and *Drosophila* TACCs. Percentages represent identities and similarities of centriolin to the homologous proteins described above. (a, bottom) Schematic showing centriolin regions predicted to be coiled coil. Below both diagrams are centriolin amino acid numbers. (b, In vitro translated) [^{35}S]methionine-labeled HA-tagged centriolin produced by in vitro translation of cDNA and resolved directly (Cen) or after immunoprecipitation with HA antibodies (Cen IP); empty vector (Vec). (b, Overexpressed) Western blots probed with anti-HA antibody showing overexpressed HA-tagged centriolin (HA-Cen) and its absence from cells overexpressing β-galactosidase (β gal). (b, Centrosome fractions) Centrosome fractions prepared from HeLa cells and *Xenopus* tissue culture (XTC) cells blotted with antibodies to centriolin (Cen) or preimmune sera (PreI). Arrowheads show position of centriolin. In XTC cells, the bands below centriolin appear to be degradation products as they are sometimes observed in protein fractions produced by in vitro translation or overexpression. Bars represent positions of molecular weight markers (×10^3). (c) Immunofluorescence images of endogenous centriolin in RPE-1 cells at different cell cycle stages. The top panels show merged images of centriolin (green), γ-tubulin (red), and nuclei (blue) from cells in G1, G2, proM (prometaphase), M (metaphase), and anaphase (A). Insets, higher magnifications of centrosomes stained for γ-tubulin (left) and centriolin (right). Centriolin localization to one of the two centrosomes is demonstrated most clearly in the G2 cell. Middle panels (Telo early) and bottom panels (Telo late) show separate images of γ-tubulin staining (left) and centriolin (right). γ-Tubulin marks both mother and daughter centrioles, which are separated in some cases. Centriolin staining is confined to one of two centrioles, which sometimes appears at the intercellular bridge (Telo early). Centrioles lacking centriolin are indicated by arrowheads in right panels. At later stages of telophase (Telo late), centriolin is also on the midbody. All immunofluorescence images (here and elsewhere) are two-dimensional projections of three-dimensional reconstructions to ensure that all stained material is visible. C, centriole; MB, midbody. Bar in c, 10 μm; but 3 μm for insets.

lapse imaging experiments showing that the maternal centriole translocates to the intercellular bridge during cytokinesis (Piel et al., 2001). Centriolin next appeared as diffusely organized material within the intercellular bridge and ultimately became concentrated at the midbody (Fig. 1 c, Telo late).

The organization of centriolin at the centrosome was more precisely determined by serum starving cells to induce growth of a primary cilium from the maternal centriole (Vorobjev and Chentsov, 1982). In these cells, centriolin staining was confined to the maternal centriole underlying the cilium (Fig. 2 b). Immunogold electron microscopy on centrosome fractions (Doxsey et al., 1994; Blomberg-Wirschell and Doxsey, 1998) confirmed localization to the maternal centriole (Fig. 2 e, M) and further demonstrated that the protein was concentrated on subdistal appendages, specialized substructures of the maternal centriole implicated in microtubule anchoring (Fig. 2, c–e) (Chretien et al., 1997; Piel et al., 2000). Based on its centriolar localization, the protein was named centriolin. Centriolin was also found at noncentrosomal apical bands of material in specialized epithelial cells that lack proteins involved in microtubule nucleation and appear to anchor the minus ends of microtubules (Mogensen et al., 1997) (Fig. 2, f and g).

Centriolin silencing by siRNA induces cytokinesis failure and a novel cytokinesis phenotype

To determine the function of centriolin, we reduced its levels using siRNAs (Fire et al., 1998; Elbashir et al., 2001). Treatment of telomerase-immortalized diploid human retinal pigment epithelial (RPE-1) cells (Morales et al., 1999) with cen-

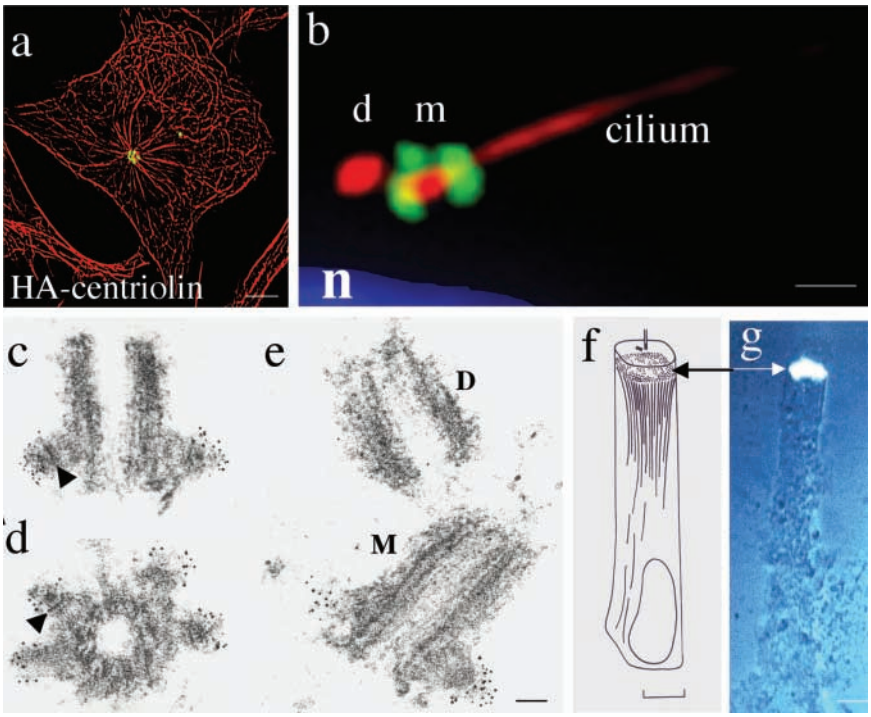

Figure 2. **Centriolin is localized to maternal centrioles and noncentrosomal sites of microtubule anchoring.** (a) HA-tagged centriolin overexpressed in COS-7 cells localizes to the centrosome (anti-HA, green) at the convergence of microtubules (red, anti–α-tubulin). (b) An RPE-1 cell immunostained with an antibody to polyglutamylated tubulin (GT335) (Bobinnec et al., 1998) to label centrioles and the primary cilium (red), and for centriolin (green), which is localized to the maternal centriole (m) associated with the primary cilium (yellow in merge) but not on the daughter centriole (d). n, nucleus. (c–e) Electron micrographs showing specific immunogold labeling of centriolin on subdistal appendages found on maternal (e, bottom, M) but not daughter centrioles (e, top, D). c and d are longitudinal and cross sections, respectively, through maternal centrioles, and e is a longitudinal section through both centrioles. Arrowheads show striations characteristic of subdistal appendages. (f and g) Centriolin is found at noncentrosomal sites of microtubule anchoring in pillar cells of the mouse cochlea (arrows) (Mogensen et al., 1997). (f) Schematic representation of a pillar cell. (g) Centriolin immunofluorescence staining overlaid with phase contrast image. Centrosome and associated cilium are shown schematically at top of cell in f. Bars: (a and g) 10 μm; (b) 2 μm; (c–e) 100 nm.

triolin-specific siRNAs caused a significant reduction in centriolin mRNA levels (Fig. 3 a). Although we were unable to examine protein levels by Western blotting of whole cell lysates due to the rare nature of this and other centrosome autoantigens (Doxsey et al., 1994), immunofluorescence staining demonstrated that centriolin was undetectable, or greatly reduced, at centrosomes in most cells (86%; $n = 1{,}012$). Quantitative analysis showed that immunofluorescence signals at individual centrosomes were significantly below those in cells treated with control lamin A/C siRNA, despite severe disruption of the nuclear lamina in the latter (Fig. 3 b) (Elbashir et al., 2001). Midbody staining of centriolin was also reduced in cells treated with siRNAs targeting centriolin.

Because centriolin shares homology with proteins known to affect microtubule organization and cytokinesis, we examined cells with reduced centriolin for defects in these functions. The most obvious cellular change detected in RPE-1 cells with reduced centriolin was a dramatic increase in the percentage of late-stage mitotic cells (~70-fold increase; Fig. 3 c). In addition, we observed an increase in the percentage of binucleate cells in three different cell lines, suggesting that a certain proportion of cells failed to cleave (Fig. 3 d; see below). The incidence of binucleate cells was significantly greater than controls, although somewhat lower than that observed for some other proteins involved in cytokinesis (Matuliene and Kuriyama, 2002; Meraldi et al., 2002; Mollinari et al., 2002). A similar cytokinesis phenotype was observed with a second set of siRNAs targeting a different centriolin sequence and with morpholino antisense DNA oligonucleotides targeting centriolin.

The dramatically high percentage of cells in late mitotic stages suggested a unique cytokinesis defect in these cells. When carefully analyzed by immunofluorescence microscopy, cells with reduced centriolin appeared to be arrested or delayed in the final stages of cytokinesis. Most cells retained intercellular bridges of varying length and thickness (Fig. 3, m and n, arrowheads). In some cases, cells remained connected even though one or both of the future daughter cells had reentered mitosis (Fig. 3 n, M). Some cells failed to cleave, forming syncytia with two, three, of four cells remaining interconnected (Fig. 3, m and n). During the early stages of cytokinesis, midbodies appeared normal.

A more complete understanding of the mechanism of cytokinesis failure was obtained by imaging live HeLa cells treated with centriolin-specific siRNAs (Fig. 4; see Videos 1–3, available at http://www.jcb.org/cgi/content/full/jcb.200301105/DC1). As expected, control cells (lamin siRNA) performed a distinct cell cleavage event with normal timing (average 2 h after mitosis) and immediately flattened and crawled apart (Fig. 4 a). Cells silenced for centriolin progressed normally through mitosis (Fig. 3, g–j; Fig. 4 e) and sometimes cleaved normally, but most failed to cleave or cleaved after prolonged periods of time (up to 23.2 h after metaphase; Fig. 4, b–d and f). These cells arrested or delayed in a unique post-telophase state. Most were unusually elongated, each with a persistent intercellular bridge of variable diameter that was often dynamic. Bridges alternated between thin threads of interconnecting cytoplasm to very thick interconnections of large diameter that appeared able to produce membrane ruffles (Fig. 4 b, 5:50, arrow). Mid-

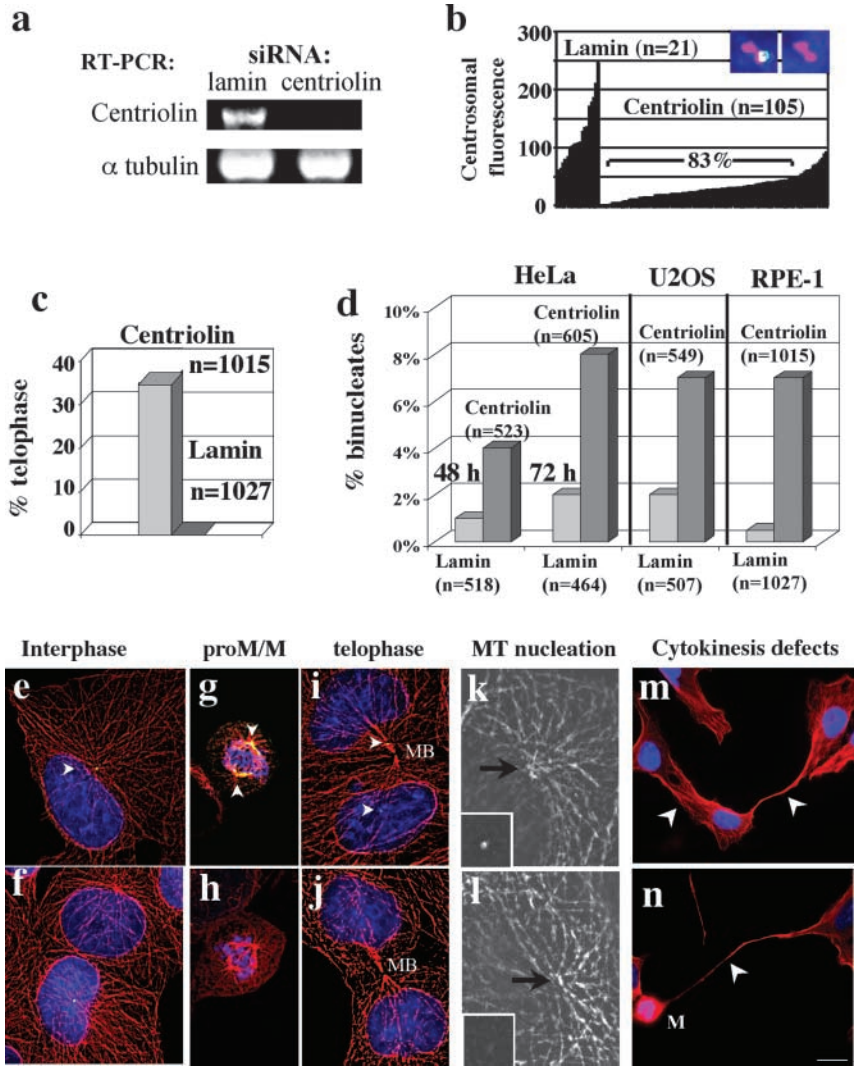

Figure 3. **RPE-1 cells treated with siRNAs targeting centriolin retain persistent intercellular connections and fail in cytokinesis.** (a) RT-PCR analysis shows that centriolin mRNA is reduced in RPE-1 cells treated with centriolin-specific siRNAs (top right) but is unaffected in cells treated with siRNAs targeting lamins A/C (top left, sequence identity confirmed). Control (α-tubulin) RT-PCR was performed in the same reaction mixtures with centriolin and lamin (bottom panels). (b) Immunofluorescence images (top right; γ-tubulin, red; centriolin, green) and quantification of centriolin levels in centrosomes from cells treated with siRNAs as indicated. The top right panel shows a cell with undetectable centriolin at the centrosome/centriole, and the top left panel shows a cell that is unaffected by the treatment and stains for centriolin (green/white). Graph shows the average centriolin fluorescence intensity/pixel at individual centrosomes (bars) in cells treated with lamin or centriolin siRNAs. The centrosome fluorescence in most centriolin siRNA–treated cells (83%) was below the lowest values observed in control cells. (c) Graph showing a dramatic increase in the percentage of cells in telophase/cytokinesis after siRNA targeting of centriolin (~70-fold). n, total number of cells counted (c and d). (d) Graph showing the increased percentage of binucleate cells in HeLa, U2OS, and RPE-1 cell lines after treatment with centriolin siRNAs (4–15-fold greater than controls). In c and d, values represent data from single experiments representative of three to four experiments. The time analyzed was as follows: HeLa, 48 h and 72 h; U2OS, 72 h; RPE-1, 24 h. (e–l) Microtubule organization (e–j) and microtubule nucleation (k and l) are not detectably altered in cells treated with centriolin siRNA (f, h, j, and l) compared with cells treated with lamin siRNA (e, g, i, and k). Arrows indicate position of centrosomes; no centrosome staining is observed in centriolin siRNA–treated cells. Insets in k and l are enlargements of centriolin staining at centrosomes (or microtubule convergence sites) at arrows. Cells in interphase (e and f, lower cell), prometaphase/metaphase (proM/M; g and h), and telophase (i and j) were labeled for microtubules (red), centrosomes (green/yellow), and nuclei (blue). MB, midbody. (m and n) Cells treated with siRNAs targeting centriolin were stained for microtubules (red) and DNA (blue). Arrowheads indicate contiguous connections between two or more cells. (m) Three interconnected cells form a syncytium. (n) One daughter of an interconnected pair of cells has reentered mitosis (M). Bar in n: (e–j) 5 μm; (k, l, and insets) 3.5 μm; (m and n) 15 μm.

bodies were not detected within persistent interconnections between cells, suggesting that they were lost sometime during the protracted period spent in cytokinesis. Interconnected cells sometimes coalesced to form single cells and then quickly moved apart again (Fig. 4 d). They sometimes made multiple failed attempts at cleavage, but in no case did we observe a cell that formed a stable binucleate. This suggested that binucleate cells observed in fixed cells (Fig. 3 d) were transient intermediates in a process that involved multiple failed attempts at cytokinesis. Cells that retained intercellular connections for long periods of time continued to progress through the cell cycle. To our surprise, some cells reentered the next mitosis while still interconnected and produced interconnected "progeny" that formed two- to four-cell syncytia, thus confirming the cell–cell interconnections observed by indirect immunofluorescence (Fig. 3, m and n). In some cases, cells that remained interconnected for long periods of time appeared to undergo apoptosis. They showed extensive blebbing, increased phase density, and decreased size and lifted from the substrate (Fig. 4 b, upper cell, 7:20).

Microtubule organization in cells with reduced centriolin appeared normal at all cell cycle stages. This included microtubules of the spindle midzone in anaphase and the midbody in telophase (Fig. 3, e–j). Microtubule nucleation from centrosomes also appeared normal (Fig. 3, k and l), although a slight delay was sometimes observed within the first minute or two. γ-Tubulin, a marker for centrosome-associated microtubule nucleation, was localized normally to centrosomes (Fig. 3 b), as were several other centrosome antigens, including GCP-2 (Murphy et al., 1998) and cNap-1 (Fry et al., 1998) (unpublished data). Midbody markers, such as anillin (see Glotzer, 2001) and γ-tubulin (Shu et al., 1995), were also localized normally. At later stages of cytoki-

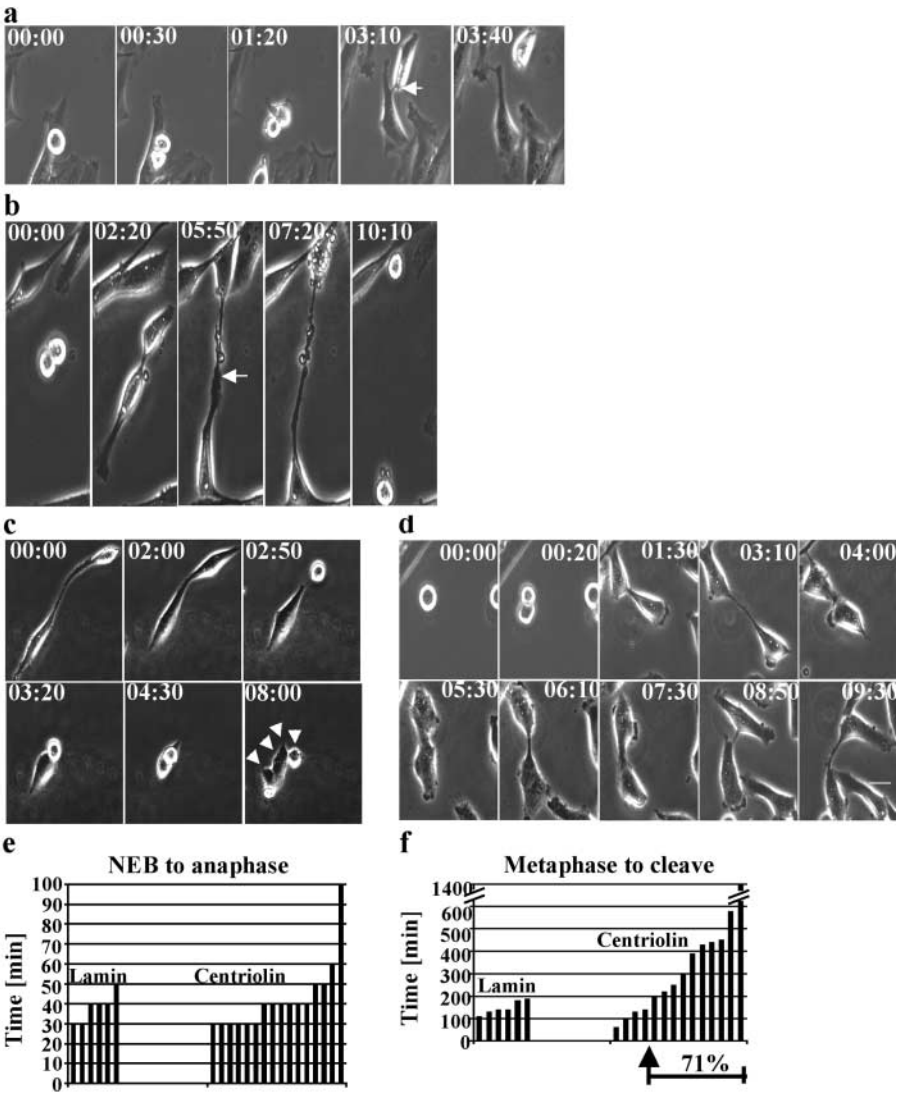

Figure 4. **Time-lapse images of HeLa cells treated with centriolin siRNAs reveal unique cytokinesis defects.** (a) A cell treated with control siRNAs targeting lamin moves apart, forms visible midbodies (arrow), and completes the final cleavage event with normal timing (1–3 h after metaphase). (b–d) Centriolin siRNA–treated cells remain attached for extended periods of time through persistent intercellular bridges and sometimes do not show visible midbodies. (b) A cell that remains attached by a long intercellular bridge for at least 8 h. The cell cleaves, both daughter cells round up, and at least one appears to undergo apoptotic cell death (upper cell, 7:20, extensive blebbing and decrease in size). (c) A dividing cell that has not completed cleavage reenters the next mitosis. One cell rounds up and is drawn to the other. The other rounds up and both undergo the early stages of cytokinesis to form a total of four cells; these progeny often remain attached by intercellular bridges forming syncytia. (d) Cell showing three failed attempts at cell cleavage over a 9.5-h time period. (e) Cells treated with siRNAs targeting centriolin progress from nuclear envelope breakdown (NEB) to anaphase with normal timing, similar to lamin siRNA controls. Vertical bars represent recordings from single cells (e and f). (f) Centriolin siRNA–treated cells are delayed in cytokinesis (~70%) compared with control lamin siRNA–treated cells, a value consistent with a 70–80% silencing efficiency. Results represent recordings of individual cells from several independent experiments. Time in hours and minutes is included in each panel in a–d. Bar, 10 μm. Time-lapse videos (Videos 1–3) of the series of images shown in a–c are available at http://www.jcb.org/cgi/content/full/jcb.200301105/DC1.

nesis in cells with long intercellular bridges, midbodies were no longer detected. These data indicate that cytokinesis failure did not result from disruption of microtubules, centrosomes, or midbodies.

Overexpression of centriolin and its Nud1 domain induces cytokinesis failure in a microtubule-independent manner

We next tested the effect of ectopic expression of centriolin and its Nud1 domain on cytokinesis and microtubule organization (Fig. 5, a–g). The most striking defects in COS-7 cells expressing HA-tagged centriolin were an increase in the proportion of telophase cells and the formation of binucleate cells (Fig. 5 g). Microtubule bundles were observed within intercellular bridges in telophase cells (Fig. 5 a), but they did not appear to cause binucleate cell formation. We found that overexpression of the 120–amino acid GFP-tagged Nud1 domain of centriolin was sufficient to induce cytokinesis failure and binucleate formation (Fig. 5, e and g) in the absence of detectable changes in microtubule organization (Fig. 5, c and d) and without disrupting endogenous centriolin from centrosomes (Fig. 5 f). The results from gene silencing and protein overexpression support a microtubule-independent mechanism for cytokinesis failure.

The centriolin Nud1 domain interacts with the yeast Bub2p in vitro

Budding yeast Nud1p anchors the MEN to the spindle pole body through direct interactions with Bub2p and perhaps other MEN components (Gruneberg et al., 2000; Pereira et al., 2000). To determine if the centriolin Nud1 homology domain (Fig. 5 h) had similar properties, we tested its ability to bind Bub2p by directed two-hybrid analysis and immunoprecipitation. Because no vertebrate Bub2p homologue has been unequivocally identified (Cuif et al., 1999), we examined the ability of the centriolin Nud1 domain to interact with yeast Bub2p. Both two-hybrid analysis and immuno-

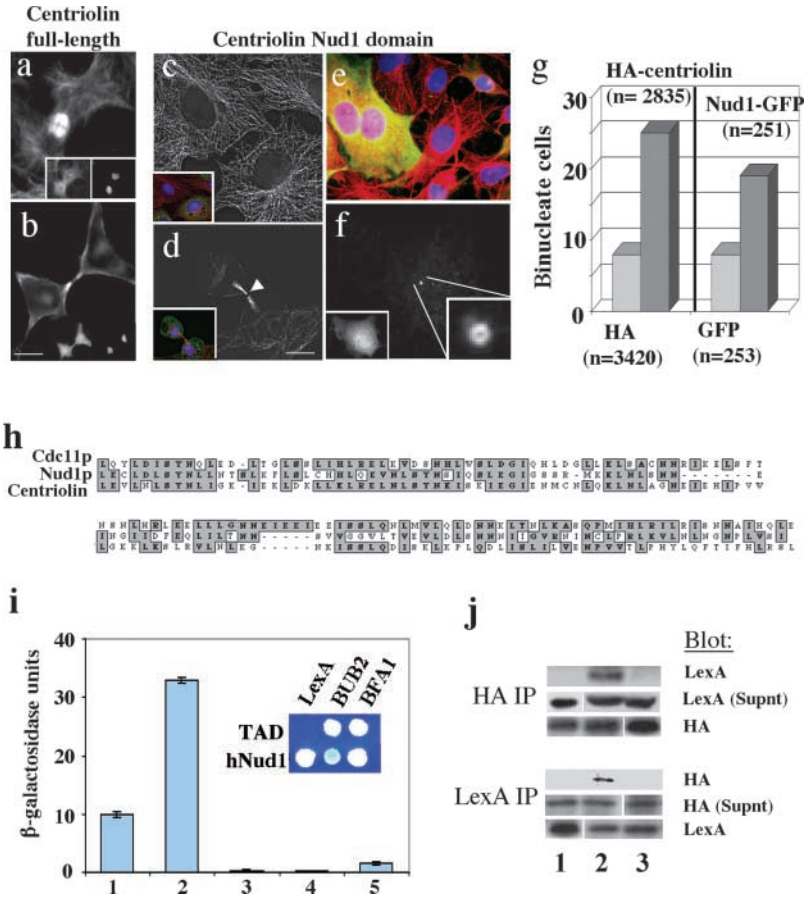

Figure 5. **Cells expressing centriolin fail in cytokinesis, as do cells expressing the centriolin Nud1 domain that interacts with yeast Bub2p.** (a) COS-7 cell overexpressing HA-tagged centriolin (left inset) showing persistent microtubule bundles in the intercellular bridge during cytokinesis (main panel, α-tubulin staining) despite reformation of the nucleus and decondensation of chromatin (DNA, right inset). (b) Control COS-7 cell (expressing HA alone, bottom center) at a similar cell cycle stage based on nuclear morphology (bottom right) shows a narrow intercellular bridge and diminished microtubule polymer (center), characteristic of cells that have reformed nuclei and decondensed DNA. (c–f) COS-7 cells expressing a GFP-tagged Nud1 domain of centriolin (c and d, insets, green; DNA, blue) have normal intercellular bridges (d, telophase, arrowhead) and normal microtubule organization (c, interphase) as in controls. However, the cells (yellow) often become binucleate (blue) by a mechanism that does not involve disruption of the endogenous centrosome-associated centriolin (f; right inset shows enlargement of centrosome, left inset shows transfected cell). (g) Quantitative analysis showing that HA–centriolin and the GFP-tagged Nud1 domain both induce significant binucleate cell formation compared with controls (HA and GFP). Values are from a single experiment and are representative of three experiments. Bar, 7 μm (for all panels). n, total number of cells counted. (h) Alignment of the centriolin Nud1 domain with the yeast Nud1p and Cdc11p proteins. (i) Direct yeast two-hybrid analysis demonstrates an interaction between the human Nud1 domain with one of the two components implicated in GTPase-activating protein activity, Bub2p, but not Bfa1p. The blue colony in the blue box and increased β-galactosidase activity (bar 2 of graph) demonstrate a specific interaction between the human centriolin Nud1 domain (hNud1) and yeast Bub2p. Bar 1, LexA–BUB2 × TAD; bar 2, LexA–BUB × TAD–hNud1; bar 3, LexA–BFA1 × TAD; bar 4, TAD–hNud1 × LexA–BFA1; bar 5, TAD-hNud1 × LexA. (j) Specific coimmunoprecipitation of HA-tagged hNud1 and LexA-tagged yeast Bub2p from yeast cells. Coprecipitation was observed using antibodies to either protein and only when both were coexpressed (top middle panel in each group). Lane 1, TAD–HA–hNud1 × LexA; lane 2, TAD–HA–hNud1 × Bub2p–LexA; lane 3, TAD–HA × Bub2p–LexA.

precipitation from yeast cells coexpressing the two proteins revealed a strong and specific interaction between the centriolin Nud1 domain and Bub2p (Fig. 5, i and j). No signal was observed when either protein was used alone, and no binding was detected between the centriolin Nud1 domain and the budding yeast MEN component Bfa1p, consistent with interaction observations in budding yeast (Pereira and Schiebel, 2001).

Cleavage failure is observed in *Xenopus* embryos injected with centriolin antibodies

A third approach was used to examine centriolin function. When affinity-purified anticentriolin antibodies (Fig. 1 b) were microinjected into one cell of two-cell *Xenopus* embryos (Doxsey et al., 1994), the injected cell failed to cleave, or cleaved a few times and then arrested; uninjected cells or preimmune IgG-injected cells divided normally (Fig. 6, a

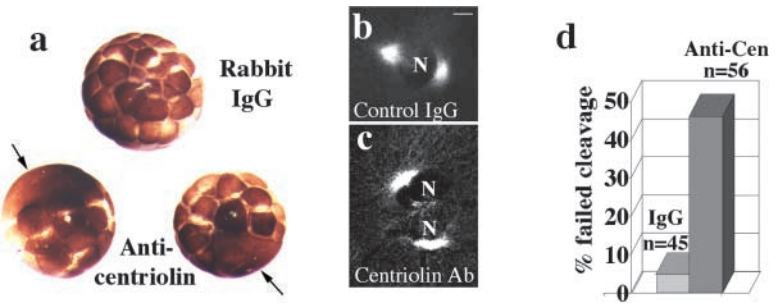

Figure 6. **Cytokinesis failure in *Xenopus* embryos injected with centriolin antibodies.** (a) *Xenopus* two-cell embryos injected into one cell with ~50 nl anti-centriolin antibodies (2 mg/ml affinity purified) fail to cleave (arrows), whereas noninjected cells (side opposite arrows) and cells injected with control rabbit IgG (2 mg/ml, top) cleave normally. (b and c) Immunofluorescence images showing two microtubule asters near a single nucleus (N) in a cell from an embryo injected with control IgG (b), and two nuclei and two asters in a cell from a centriolin antibody–injected cell (c, microtubules stained with anti–α-tubulin). Bar, 10 μm (for b and c). (d) Quantification of results from injection experiments showing an approximately eight-fold increase in cleavage failure (representative of three experiments). n, number of embryos examined.

and d). Centriolin antibody–injected cells arrested with two nuclei and two well-organized microtubule asters, indicating that karyokinesis and microtubule organization were normal, but cells failed to complete the final event of mitosis, cell cleavage (Fig. 6 c). Preimmune IgG-injected cells had a single nucleus with one or two microtubule asters, depending on their cell cycle stage, as would be expected for cells that had undergone normal cell cleavage (Fig. 6 b). Taken together, the results from gene silencing, antibody injection, and protein overexpression in several experimental systems all demonstrate that centriolin plays an important role in the late stages of cytokinesis.

siRNA-induced gene silencing of centriolin causes G1/G0 arrest

Cytokinesis defects and delays induced by centriolin silencing were observed at early times after treatment of RPE-1 cells (18–24 h). At later times (48–72 h after treatment), a reduction in the mitotic index was observed, suggesting that the cells were arrested at some other stage of the cell cycle. This was directly tested by treating cells with nocodazole to induce mitotic arrest and quantifying mitotic cells in DAPI-stained preparations. Under these conditions, most lamin siRNA–treated control RPE-1 cells were arrested in mitosis (71%), whereas only a small fraction of centriolin siRNA–treated cells arrested at this cell cycle stage (<1%). To determine the cell cycle stage of arrest, cells were analyzed by flow cytometry. In the presence of nocodazole, control cells showed a significant shift from the G1 peak to the G2/M peak (Fig. 7 a, red). In contrast, cells treated with siRNAs targeting centriolin did not significantly shift into the G2/M peak in the presence of nocodazole but remained largely in G1 (Fig. 7 a, blue). The inability to undergo a nocodazole-induced shift into the G2/M peak was a feature shared by cells driven into G0 by serum starvation (Fig. 7 b, blue). The proportion of cells in S phase was either unaltered or slightly decreased in cells silenced for centriolin both in the presence of nocodazole (centriolin, 13%; lamin, 23%) or in its absence (centriolin, 13%; lamin, 19%). These results demonstrate that cells with reduced centriolin arrest before S phase, possibly in G1/S, G1, or G0.

Ki-67 staining was also used to examine the stage of cell cycle arrest. Ki-67 is an antibody directed against a nuclear protein that stains cycling cells or cells arrested in cycle (e.g., G1/S or S phase; Gerdes et al., 1984) but not cells that are quiescent (G0) or differentiated. As expected, nearly all untreated RPE-1 cells or control cells treated with siRNAs targeting GFP or lamins A/C were positive for Ki-67 (Fig. 7, c and d). However, most cells with reduced centriolin had undetectable levels of Ki-67 staining (Fig. 7, c and d). Taken together, results from mitotic index assays, flow cytometry, and Ki-76 staining in RPE-1 and HME-1 (human mammary epithelia) cells (unpublished data) demonstrated that reduction of centriolin levels prevented cells from entering S phase and appeared to drive them out of cycle into a G0-like state. This cell cycle arrest effectively prevents the initiation of additional rounds of centrosome duplication in cells compromised by having diminished levels of centriolin.

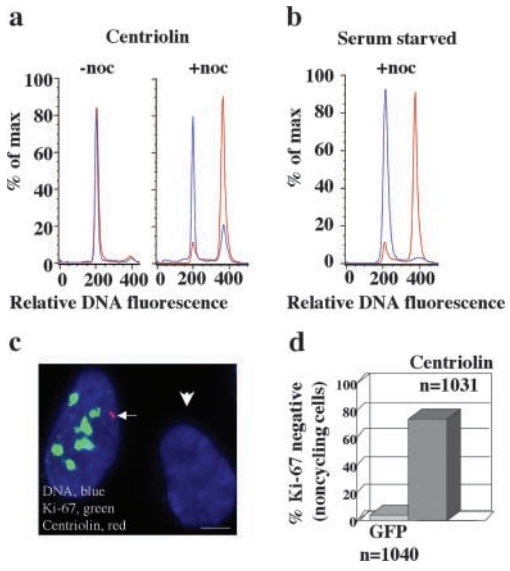

Figure 7. **siRNAs targeting centriolin induce G1/G0 arrest.** (a) RPE-1 cells treated with centriolin siRNAs (blue) do not shift into the G2/M peak after nocodazole treatment as seen for control lamin siRNA–treated cells (red). (b) The inability of cells treated with centriolin siRNAs to shift into the G2/M peak is similar to that observed in serum-starved cells (blue, serum starved; red, not starved). (c) Ki-67 staining of control cells (left cell, green) occurs together with centriolin staining (left cell, red at arrow); both are gone in centriolin siRNA–treated cells (right, arrowhead). Bar, 7.5 μm. (d) Cells treated with siRNAs targeting centriolin lack Ki-67 staining (~70%), whereas most control cells stain positively (GFP siRNAs). a, b, and d are representative experiments from five experiments for a, two for b, and three for d. n, total number cells counted.

Discussion

In this paper, we characterize centriolin, a maternal centriole component whose disruption induces cytokinesis failure and G1/G0 arrest. The ability of centriolin to induce this phenotype may provide a molecular explanation for the cytokinesis defects and G1 arrest previously observed in vertebrate cells after experimental removal of entire centrosomes (Hinchcliffe et al., 2001; Khodjakov and Rieder, 2001). Moreover, association of centriolin with the maternal centriole may be a molecular requirement for activation and completion of the final stages of cytokinesis, functions recently suggested for the maternal centriole in vertebrate cells (Piel et al., 2001).

The cytokinesis phenotype observed in cells treated with siRNAs targeting centriolin is uncommon among proteins that function in cytokinesis. The predominant phenotype observed after functional abrogation of most proteins that cause cytokinesis failure is coalescence of dividing cells into a single cell with two nuclei. This has been shown for proteins of the central spindle, regulatory proteins that control cytokinesis, microtubule-associated proteins, and the centrosome proteins γ-tubulin and centrin (Shu et al., 1995; Kaiser et al., 2002; Manabe et al., 2002; Matuliene and Kuriyama, 2002; Meraldi et al., 2002; Mollinari et al., 2002; Salisbury et al., 2002; Seong et al., 2002). In contrast, the predominant cytokinesis phenotype observed in cells with reduced centriolin is failure to resolve persistent intercellular bridges

between dividing cells. The apparent consequences of this event are generation of multicellular syncytia, continuous attempts at cell cleavage that include binucleate cells as intermediates, completion of cytokinesis, perhaps artificially, by traction-mediated cytokinesis (Burton and Taylor, 1997), and apoptotic cell death. Although we have not determined the precise mechanism of cytokinesis failure in cells with abrogated centriolin function, we are testing whether membrane is incorporated normally into the cleavage site (Finger and White, 2002; Thompson et al., 2002).

Persistent intercellular bridges have also been observed between dividing vertebrate cells overexpressing the Cdc14A phosphatase (Kaiser et al., 2002). This uncommon phenotype has thus far been observed only with proteins (centriolin and Cdc14A) that share homology with components of yeast regulatory pathways that control mitotic exit and cytokinesis (MEN/SIN) and localize to the same intracellular sites as the yeast proteins (centrosome/spindle pole bodies). Persistent intercellular connections may also be present in cells lacking centrosomes and may reflect a similar type of cytokinesis defect (Doxsey, 2001a). Although the mechanism of cytokinesis failure appears to be different in SIN mutants, the outcome is the same, production of bi- and multinucleate cells. These observations support the idea that vertebrate cells may possess regulatory pathways that function in much the same way as those in yeast to coordinate the final stages of cytokinesis with chromosome segregation.

Several domains of centriolin share sequence homology with proteins implicated in tumorigenesis, including the TACCs and oncoprotein 18/stathmin. In this paper, we show that the domain homologous to Nud1p/Cdc11p can induce aneuploidy through cytokinesis failure. This event could generate further genetic instability through the organization of multipolar spindles by supernumerary centrosomes and could thus facilitate the accumulation of activated oncogenes and loss of tumor suppressor genes (Pihan et al., 2001; Doxsey, 2002). We are currently investigating the role of centriolin in human oncogenesis.

Our results suggest that minor changes in centrosome composition, such as loss of centriolin, can arrest cells in G1/G0. Because cells with reduced centriolin have difficulty completing the final stages of cytokinesis, it is tempting to suggest that G1/G0 arrest is a consequence of improper cytokinesis. However, it has been suggested that G1 arrest in cells lacking centrosomes may also result from the loss of core centrosome components, improper spindle alignment, or the presence of excess DNA in binucleate cells (Andreassen et al., 2001; Hinchcliffe et al., 2001; Khodjakov and Rieder, 2001; Meraldi et al., 2002). We are currently testing a model in which the loss of core centrosome components activates a checkpoint involved in monitoring "centrosome integrity" and thus prevents centrosome duplication by arresting cells in G1/G0, as we and others have proposed (Doxsey, 2001a; Quintyne and Schroer, 2002).

Materials and methods

Cell culture and transfections

The cells used primarily in this study were diploid, telomerase-immortalized human RPE-1 cells (hTERT–RPE-1s; CLONTECH Laboratories, Inc.) (Morales et al., 1999). Other cells included HeLa, COS-7, hTERT–HME-1 (human mammary epithelia), U2OS, and *Xenopus* tissue culture (XTC) cells. All were grown as previously described (American Type Culture Collection). COS-7 cells were transfected as previously described (Lipofectamine; Invitrogen).

Antibodies

Amino acids 268–903 or centriolin were fused with GST (CLONTECH Laboratories, Inc.), overexpressed in *Escherichia coli*, and purified as previously described (Doxsey et al., 1994). Antibodies raised in rabbits were affinity purified by passing sera over a GST column to remove anti-GST antibodies and then over a GST–centriolin column. Antibodies to the following proteins were also used in this study: lamin A/C (Cell Signaling Technology), α- and γ-tubulins (Sigma-Aldrich), LexA (Santa Cruz Biotechnology, Inc.), GAL4 transactivation domain (TAD) (CLONTECH Laboratories, Inc.), Ki-67, and HA (BD Biosciences).

Immunofluorescence and electron microscopy

Cells were prepared for immunofluorescence, imaged, and deconvolved (Metamorph; Universal Imaging Corp.), and centrosomes were quantified as previously described (Dictenberg et al., 1998). All immunofluorescence images are two-dimensional projections of three-dimensional reconstructions to ensure that all stained material was visible in two-dimensional images. Immunogold electron microscopy was performed as previously described (Doxsey et al., 1994) using centrosome fractions from HeLa cells (Blomberg-Wirschell and Doxsey, 1998) and antibodies to centriolin followed by antibodies coupled to 5-nm gold particles (Amersham Biosciences). Pillar cells were prepared and stained as previously described (Mogensen et al., 1997).

Centriolin cloning

A cDNA of ~1.7 kb was identified by screening a human placenta expression library with serum from individuals with scleroderma (Doxsey et al., 1994). The nucleotide sequence was compared with others (blastn) in the human genome database (National Center for Biotechnology Information) and revealed a sequence with 99% identity on chromosome 9 q34.11–34.13. Genscan predicted an ~7-kb gene comprising 40 exons. PCR primers were used to obtain an ~7-kb cDNA in a human testes cDNA library. The 5′ end, obtained by rapid amplification of cDNA ends (RACE), was identical to the predicted sequence. A full-length HA-tagged centriolin was obtained by inserting an HA tag (YPYDVPDYASL) 5′ to the RACE fragment and ligating the HA–centriolin cDNA to the original fragment. The full-length centriolin cDNA contained 6,975 nucleotides with an ORF of 2,325 amino acids and predicted a molecular mass of 269 kD, consistent with the molecular mass of endogenous centriolin (Fig. 1).

Regions flanking the ORF had a translational start (Kozak sequence), polyadenylation sequence, poly-A tail, and multiple upstream and downstream stop codons. The construct was inserted into pcDNA 3.1 Zeo (+) (Invitrogen) using BamHI and NotI restriction sites. Centriolin was translated in vitro (TNT; Promega) and expressed in cultured cells using conventional procedures (Lipofectamine). Centriolin amino acids 435–623 and 1385–1658 were 24% identical/47% similar and 20% identical/41% similar to the COOH-terminal half of TACCs, respectively. Amino acids 879–913 were 40% identical/51% similar to amino acids 72–106 of human stathmin. Amino acids 126–234 were 31–35% identical/47–50% similar to Nud1p and Cdc11p.

siRNAs and morpholino antisense

siRNAs targeting centriolin, lamin A/C, and GFP mRNAs were made as complimentary single-stranded 19-mer siRNAs with 3′ dTdT overhangs (Dharmacon Research), deprotected, annealed, and delivered into cells using a 400 μM stock (Oligofectamine; Invitrogen). The nucleotides targeted were as follows: in centriolin, 117–136 and 145–163; in lamin A/C, 608–630; and in pEGFP-C1 (CLONTECH Laboratories, Inc.), 233–252.

Fluorescein-conjugated morpholino antisense DNA oligonucleotides (Gene Tools) targeting the start codon of centriolin were introduced into cells using the EPEI agent (Gene Tools). The inverse sequence was used as control.

Time-lapse imaging

HeLa cells plated on coverslips (25 mm diameter) were treated with siRNAs targeting centriolin for 50 h. They were placed in a chamber (PDMI-2; Harvard Apparatus) in complete medium with CO_2 exchange (0.5 liters/min) at 37°C. Cells were imaged every 10 min for 12–20 h using a 20× or 40× phase contrast lens with a green interference filter on an inverted microscope (Olympus IX-70). Images were captured on a CoolSnap HQ CCD

camera (Roper Scientific) and concatenated using Metamorph software (Universal Imaging Corp.).

Primary cilium formation and microtubule nucleation

Primary cilia were induced by culturing hTERT–RPE-1 cells in medium with 0.25% serum for 48 h and identified using the GT335 antibody raised to polyglutamylated α- and β-tubulins (Bobinnec et al., 1998). Microtubule nucleation was performed as previously described (Purohit et al., 1999) by treatment with nocodazole (1 mg/ml) for 1 h at 37°C, fixing cells at various times after washing out drug, and then staining for microtubules.

RT-PCR

Centriolin mRNA levels were assayed by RT-PCR using 10 μl mRNA (OneStep RT-PCR; QIAGEN); α-tubulin served as an internal control in the same reaction. All products were sequenced.

Yeast two-hybrid analysis and immunoprecipitations

A fragment containing amino acids 127–233 of centriolin was cloned into EcoRI and SalI sites of pGADT7 (CLONTECH Laboratories, Inc.) to produce a fusion with the GAL4 TAD. Constructs pEG202 (LexA), pGP69 (LexA-*BUB2*), and pGP122 (LexA-*BFA1*) and the yeast strain SGY37 were from Elmar Schiebel (Paterson Institute for Cancer Research, Manchester, UK). SGY37, which contains a *LacZ* reporter gene under the control of a LexA operator, was transformed with plasmid DNA using LiAc (Ito et al., 1983), and transformants were selected for on dropout medium. We used semiquantitative β-galactosidase assays (Schramm et al., 2001) and more quantitative β-galactosidase assays with CPRG (chlorophenol red-β-D-galactopyranoside; Roche) as a substrate per the manufacturer's instructions. Coimmunoprecipitation of LexA and GAL4 TAD fusion proteins was performed as previously described (Schramm et al., 2001).

Flow cytometry

Cells treated with siRNAs for 50–70 h were treated with 100 ng/ml for 12 h, removed from plates, and fixed in methanol. Cells stained with propidium iodide were analyzed by flow cytometry (FACSCAN®; Becton Dickinson) using Flojo software (Tree Star, Inc.).

GenBank/EMBL/DDBJ accession numbers

The GenBank/EMBL/DDBJ accession number for centriolin is AF513978 and for lamin A/C is X03444.

Online supplemental material

Supplemental videos (Videos 1–3) are available at http://www.jcb.org/cgi/content/full/jcb.200301105/DC1. The supplemental videos show that cells silenced for centriolin delay in cytokinesis, remain interconnected by persistent intercellular bridges, re-enter mitosis while still interconnected, and form multicellular syncytia. Some cells divide normally while others undergo apparent apoptosis characterized by blebbing, rounding up, diminution in size, and loss of substrate attachment.

We wish to thank Yu-Li Wang, Dannel McCollum, Kip Sluder, Bill Theurkauf, and Nick Rhind for scientific discussion and critical reading of the manuscript. We thank Cytomyx for assistance in the cloning of centriolin, Irina Gavanescu for help with PCR, Phillipe Denoulet (Université Pierre et Marie Curie, Paris, France) for GT335 antibodies, E. Schiebel for yeast constructs, Chris Powers for assistance with electron microscopy, and J. McClean for construction of the human placenta cDNA expression library.

This work was supported by grants from the National Institutes of Health (GM-51994 and CA82834) and the Department of Defense (DAMD17-98-1-8521) to S. Doxsey.

Submitted: 27 January 2003
Revised: 6 March 2003
Accepted: 10 March 2003

References

Andersen, S.S. 2000. Spindle assembly and the art of regulating microtubule dynamics by MAPs and Stathmin/Op18. *Trends Cell Biol.* 10:261–267.

Andreassen, P.R., O.D. Lohez, F.B. Lacroix, and R.L. Margolis. 2001. Tetraploid state induces p53-dependent arrest of nontransformed mammalian cells in G1. *Mol. Biol. Cell.* 12:1315–1328.

Bardin, A.J., and A. Amon. 2001. Men and sin: what's the difference? *Nat. Rev. Mol. Cell Biol.* 2:815–826.

Blomberg-Wirschell, M., and S.J. Doxsey. 1998. Rapid isolation of centrosomes. *Methods Enzymol.* 298:228–238.

Bobinnec, Y., A. Khodjakov, L.M. Mir, C.L. Rieder, C.L. Edde, and M. Bornens. 1998. Centriole disassembly in vivo and its effect on centrosome structure and function in vertebrate cells. *J. Cell Biol.* 143:1575–1589.

Burton, K., and D.L. Taylor. 1997. Traction forces of cytokinesis measured with optically modified elastic substrata. *Nature.* 385:450–454.

Chretien, D., B. Buendia, S.D. Fuller, and E. Karsenti. 1997. Reconstruction of the centrosome cycle from cryoelectron micrographs. *J. Struct. Biol.* 120: 117–133.

Cuif, M.H., F. Possmayer, H. Zander, N. Bordes, F. Jollivet, A. Couedel-Courteille, I. Janoueix-Lerosey, G. Langsley, M. Bornens, and B. Goud. 1999. Characterization of GAPCenA, a GTPase activating protein for Rab6, part of which associates with the centrosome. *EMBO J.* 18:1772–1782.

Dictenberg, J., W. Zimmerman, C. Sparks, A. Young, C. Vidair, Y. Zheng, W. Carrington, F. Fay, and S.J. Doxsey. 1998. Pericentrin and γ-tubulin form a protein complex and are organized into a novel lattice at the centrosome. *J. Cell Biol.* 141:163–174.

Doxsey, S. 2002. Duplicating dangerously: linking centrosome duplication and aneuploidy. *Mol. Cell.* 10:439–440.

Doxsey, S.J. 2001a. Centrosomes as command centres for cellular control. *Nat. Cell Biol.* 3:E105–E108.

Doxsey, S.J. 2001b. Re-evaluating centrosome function. *Nat. Rev. Mol. Cell Biol.* 2:688–698.

Doxsey, S.J., P. Stein, L. Evans, P. Calarco, and M. Kirschner. 1994. Pericentrin, a highly conserved protein of centrosomes involoved in microtubule orgainzation. *Cell.* 76:639–650.

Elbashir, S.M., J. Harborth, W. Lendeckel, A. Yalcin, K. Weber, and T. Tuschl. 2001. Duplexes of 21-nucleotide RNAs mediate RNA interference in cultured mammalian cells. *Nature.* 411:494–498.

Finger, F.P., and J.G. White. 2002. Fusion and fission: membrane trafficking in animal cytokinesis. *Cell.* 108:727–730.

Fire, A., S. Xu, M.K. Montgomery, S.A. Kostas, S.E. Driver, and C.C. Mello. 1998. Potent and specific genetic interference by double-stranded RNA in *Caenorhabditis elegans*. *Nature*. 391:806–811.

Fry, A.M., T. Mayor, P. Meraldi, Y.D. Stierhof, K. Tanaka, and E.A. Nigg. 1998. C-Nap1, a novel centrosomal coiled-coil protein and candidate substrate of the cell cycle–regulated protein kinase Nek2. *J. Cell Biol.* 141:1563–1574.

Gerdes, J., H. Lemke, H. Baisch, H.H. Wacker, U. Schwab, and H. Stein. 1984. Cell cycle analysis of a cell proliferation-associated human nuclear antigen defined by the monoclonal antibody Ki-67. *J. Immunol.* 133:1710–1715.

Glotzer, M. 2001. Animal cell cytokinesis. *Annu. Rev. Cell Dev. Biol.* 17:351–386.

Gruneberg, U., K. Campbell, C. Simpson, J. Grindlay, and E. Schiebel. 2000. Nud1p links astral microtubule organization and the control of exit from mitosis. *EMBO J.* 19:6475–6488.

Guasch, G., G.J. Mack, C. Popovici, N. Dastugue, D. Birnbaum, J.B. Rattner, and M.J. Pebusque. 2000. FGFR1 is fused to the centrosome-associated protein CEP110 in the 8p12 stem cell myeloproliferative disorder with t(8;9)(p12; q33). *Blood.* 95:1788–1796.

Guertin, D.A., S. Trautmann, and D. McCollum. 2002. Cytokinesis in eukaryotes. *Microbiol. Mol. Biol. Rev.* 66:155–178.

Hinchcliffe, E.H., F.J. Miller, M. Cham, A. Khodjakov, and G. Sluder. 2001. Requirement of a centrosomal activity for cell cycle progression through G1 into S phase. *Science.* 291:1547–1550.

Ito, H., Y. Fukuda, K. Murata, and A. Kimura. 1983. Transformation of intact yeast cells treated with alkali cations. *J. Bacteriol.* 153:163–168.

Kaiser, B.K., Z.A. Zimmerman, H. Charbonneau, and P.K. Jackson. 2002. Disruption of centrosome structure, chromosome segregation, and cytokinesis by misexpression of human Cdc14A phosphatase. *Mol. Biol. Cell.* 13:2289–2300.

Khodjakov, A., and C.L. Rieder. 2001. Centrosomes enhance the fidelity of cytokinesis in vertebrates and are required for cell cycle progression. *J. Cell Biol.* 153:237–242.

Lange, B.M., and K. Gull. 1995. A molecular marker for centriole maturation in the mammalian cell cycle. *J. Cell Biol.* 130:919–927.

Lee, M.J., F. Gergely, K. Jeffers, S.Y. Peak-Chew, and J.W. Raff. 2001. Msps/XMAP215 interacts with the centrosomal protein D-TACC to regulate microtubule behaviour. *Nat. Cell Biol.* 3:643–649.

Lupas, A., M. VanDyke, and J. Stock. 1991. Predicting coiled-coils from protein sequences. *Science.* 252:1162–1164.

Manabe, R., L. Whitmore, J.M. Weiss, and A.R. Horwitz. 2002. Identification of a

novel microtubule-associated protein that regulates microtubule organization and cytokinesis by using a GFP-screening strategy. *Curr. Biol.* 12:1946–1951.

Matuliene, J., and R. Kuriyama. 2002. Kinesin-like protein CHO1 is required for the formation of midbody matrix and the completion of cytokinesis in mammalian cells. *Mol. Biol. Cell.* 13:1832–1845.

McCollum, D., and K.L. Gould. 2001. Timing is everything: regulation of mitotic exit and cytokinesis by the MEN and SIN. *Trends Cell Biol.* 11:89–95.

Meraldi, P., R. Honda, and E.A. Nigg. 2002. Aurora-A overexpression reveals tetraploidization as a major route to centrosome amplification in $p53^{-/-}$ cells. *EMBO J.* 21:483–492.

Mogensen, M.M., J.B. Mackie, S.J. Doxsey, T. Stearns, and J.B. Tucker. 1997. Centrosomal deployment of γ-tubulin and pericentrin: evidence for a microtubule-nucleating domain and a munis-end docking domain in certain mouse epithelial cells. *Cell Motil. Cytoskeleton.* 36:276–290.

Mogensen, M.M., A. Malik, M. Piel, V. Bouckson-Castaing, and M. Bornens. 2000. Microtubule minus-end anchorage at centrosomal and non-centrosomal sites: the role of ninein. *J. Cell Sci.* 113:3013–3023.

Mollinari, C., J.P. Kleman, W. Jiang, G. Schoehn, T. Hunter, and R.L. Margolis. 2002. PRC1 is a microtubule binding and bundling protein essential to maintain the mitotic spindle midzone. *J. Cell Biol.* 157:1175–1186.

Morales, C.P., S.E. Holt, M. Ouellette, K.J. Kaur, Y. Yan, K.S. Wilson, M.A. White, W.E. Wright, and J.W. Shay. 1999. Absence of cancer-associated changes in human fibroblasts immortalized with telomerase. *Nat. Genet.* 21:115–118.

Murphy, S.M., L. Urbani, and T. Stearns. 1998. The mammalian γ-tubulin complex contains homologues of the yeast spindle pole body components spc97p and spc98p. *J. Cell Biol.* 141:663–674.

Pereira, G., and E. Schiebel. 2001. The role of the yeast spindle pole body and the mammalian centrosome in regulating late mitotic events. *Curr. Opin. Cell Biol.* 13:762–769.

Pereira, G., T. Hofken, J. Grindlay, C. Manson, and E. Schiebel. 2000. The Bub2p spindle checkpoint links nuclear migration with mitotic exit. *Mol. Cell.* 6:1–10.

Piel, M., P. Meyer, A. Khodjakov, C.L. Rieder, and M. Bornens. 2000. The respective contributions of the mother and daughter centrioles to centrosome activity and behavior in vertebrate cells. *J. Cell Biol.* 149:317–330.

Piel, M., J. Nordberg, U. Euteneuer, and M. Bornens. 2001. Centrosome-dependent exit of cytokinesis in animal cells. *Science.* 291:1550–1553.

Pihan, G.A., A. Purohit, J. Wallace, R. Malhotra, L. Liotta, and S.J. Doxsey. 2001. Centrosome defects can account for cellular and genetic changes that characterize prostate cancer progression. *Cancer Res.* 61:2212–2219.

Purohit, A., S.H. Tynan, R. Vallee, and S.J. Doxsey. 1999. Direct interaction of pericentrin with cytoplasmic dynein light intermediate chain contributes to mitotic spindle organization. *J. Cell Biol.* 147:481–491.

Quintyne, N.J., and T.A. Schroer. 2002. Distinct cell cycle–dependent roles for dynactin and dynein at centrosomes. *J. Cell Biol.* 159:245–254.

Rappaport, R. 1986. Establishment of the mechanism of cytokinesis in animal cells. *Int. Rev. Cytol.* 105:245–281.

Salisbury, J.L., K.M. Suino, R. Busby, and M. Springett. 2002. Centrin-2 is required for centriole duplication in mammalian cells. *Curr. Biol.* 12:1287–1292.

Schramm, C., C. Janke, and E. Schiebel. 2001. Molecular dissection of yeast spindle pole bodies by two hybrid, in vitro binding, and co-purification. *Methods Cell Biol.* 67:71–94.

Seong, Y.S., K. Kamijo, J.S. Lee, E. Fernandez, R. Kuriyama, T. Miki, and K.S. Lee. 2002. A spindle checkpoint arrest and a cytokinesis failure by the dominant-negative polo-box domain of Plk1 in U-2 OS cells. *J. Biol. Chem.* 277:32282–32293.

Shu, H.B., Z. Li, M.J. Palacios, Q. Li, and H.C. Joshi. 1995. A transient association of γ-tubulin at the midbody is required for the completion of cytokinesis during the mammalian cell division. *J. Cell Sci.* 108:2955–2962.

Thompson, H.M., A.R. Skop, U. Euteneuer, B.J. Meyer, and M.A. McNiven. 2002. The large GTPase dynamin associates with the spindle midzone and is required for cytokinesis. *Curr. Biol.* 12:2111–2117.

Vorobjev, I.A., and Y.S. Chentsov. 1982. Centrioles in the cell cycle. I. Epithelial cells. *J. Cell Biol.* 93:938–949.